DEVELOPMENT OF A REDUCED COMBUSTION MECHANISM FOR 2-BUTYLTETRAHYDROFURAN AND ITS BLENDS WITH DIESEL

Qingfeng ZHANG *, ***Konghao CHEN, Yingjun YU, and Heng LU***

College of Mechanical and Electrical Engineering, Wenzhou University, Wenzhou, China

Corresponding author; E-mail: qingfeng1204@163.com

2-Butyltetrahydrofuran is being investigated as a potential alternative fuel for diesel engines due to its self-ignition properties. This paper presents a reduced 2-butyltetrahydrofuran chemical kinetic mechanism for the first time, accompanied by an in-depth study of its combustion characteristics. N-heptane/toluene is a recognized surrogate mixture that effectively represents complex diesel for analyzing combustion behaviors. To achieve optimal combustion and application of 2-BTHF in diesel blends, this paper introduces a reliable mechanism for the 2-BTHF/n-heptane/toluene mixture for the first time. Firstly, directed relation graphs with error propagation, combined with isomer lumping and sensitivity analysis, are proposed to efficiently reduce detailed mechanisms, enhancing the approximation process in mechanism establishment. Results from the reduced 2-BTHF mechanism show that the cooperative methodology effectively diminishes the complexity of the detailed mechanism while improving its predictive capabilities. Secondly, the reduced 2-BTHF mechanism is combined and refined with those of n-heptane and toluene. Its accuracy is verified using diverse experimental data, including ignition delay times from shock tubes/rapid compressors and laminar flame speeds measured in combustion vessels. The final reduced chemical kinetic mechanism for the mixture comprises 78 species and 300 reactions, demonstrating significant potential for simulating the combustion behavior of 2-BTHF/n-heptane/toluene blends. Additionally, the study explores the impact of adding 2-BTHF to diesel fuel. Results reveal that increasing the proportion of blended 2-BTHF gradually raises the laminar flame speeds of diesel, while having minimal influence on ignition delay times.

Key words*: 2-butyltetrahydrofuran, self-ignition, n-heptane, toluene, reduced mechanism, blended*

1. Introduction

Internal combustion engines (ICEs) hold a dominant position in automotive propulsion systems and stationary energy infrastructure, attributed to thermodynamic efficiency, high volumetric energy density, and operational reliability. However, the fossil fuel crisis and environmental protection concerns have prompted engine researchers to actively seek out alternative fuels [1-3]. The application of alternative fuels serves as an effective strategy to mitigate CO_2 emissions from transport-based facilities. Among the numerous alternative fuels available, hydrogen and ammonia are prominent candidates. Despite their potential for direct use in maritime and road transportation, their widespread adoption has yet to be realized. This is mainly due to stringent storage conditions required for hydrogen and inherent challenges associated with igniting ammonia [4, 5]. Biofuels, as an alternative, typically exhibit superior ignition characteristics and greater compatibility with existing fuel storage and distribution systems. Furthermore, they can be easily integrated into current internal combustion engine systems [6-8]. Among them, saturated furans, inedible crop and plant materials composed of lignocellulose, are mainly produced through the catalytic conversion of cellulosic biomass and are considered as promising biomass resources [9]. Due to their physical and chemical properties that closely resemble those of conventional fuels, they have emerged as potential substitutes or additives for gasoline and diesel. Currently, the development and validation of reduced mechanisms for furan-based biofuel blends for diesel engines has become a research hotspot. Wei *et al.* [10] constructed a reduced mechanism for 2-methylfuran/biodiesel blends aiming to optimize their combustion characteristics in diesel engines, while Zhang *et al.* [11] focused on the mechanism construction and validation of 2-methylfuran-diesel blends. These studies provide important references for understanding the interaction and combustion behavior of biofuels and diesel. In research on the ignition behavior of saturated furans, researchers have found that the length of their side chains significantly impacts their ignition characteristics, which in turn determines their potential applications [12]. Specifically, 2-butyltetrahydrofuran (2-BTHF), a saturated furan with a long side chain, has physicochemical properties highly similar to those of diesel fuel. This similarity renders 2-BTHF a highly promising renewable biofuel for ICEs, presenting broad prospects for its utilization in the future. In our previous work [13], we have already partially explored the relevant aspects of 2-BTHF and its blends with other fuels. Building upon this foundation, the present study aims to further advance the research in this area.

As a potential bio-based fuel, the physicochemical properties of 2-BTHF are very close to those of traditional diesel. From the perspective of ignition performance index, the standard reference value describing the ignition behavior of fuel in compression ignition engine is derived cetane number (DCN), and the DCN of traditional diesel is between 40 and 55 [12, 14, 15]. The DCN of 2-BTHF is 45.5, which is very close to the DCN of diesel, indicating that the two have considerable self-ignition ability during the compression ignition process and can meet the basic requirements of the engine for fuel ignition delay. Furthermore, the molecular structure of 2-BTHF contains C-O bonds and has an oxygen content of 12.9% by weight. This can potentially enhance the combustion process and reduce the particulate matter emissions in compression ignition engines [16]. Previous assessments of tetrahydrofuran fuels in ICEs have been revealed satisfactory power outputs and emission levels [17]. Considering these factors, 2-BTHF appears to be a highly promising candidate for meeting the requirements of alternative diesel fuels. Its properties suggest that it could be implemented in various applications where diesel is currently used, although further research may be required to optimize its performance and ensure seamless integration into existing engine systems.

In the current research on 2-BTHF, Cai *et al.* [14] were the first to develop a detailed kinetic mechanism for the combustion of 2-BTHF to describe its oxidation at low and high temperatures, which including 424 species and 1790 reactions. This mechanism can well predict the laminar flame speed data of 2-BTHF measured under pressures of 1-3 atm (1 atm=101,325 kPa) , temperature of 448K , and equivalence ratios (Ratio of the amount of air required for complete combustion of the fuel to the actual amount of air supplied) of 0.6-1.4 in a high-pressure combustion vessel, and the ignition delay time data measured under pressures of 10 and 20 atm, temperature of 660-1250K and an equivalence ratio of 1 in a Shock tube (ST) and a rapid compressor (RCM). However, the scale of the mechanism is too large and requires too much computing time to be useful in 3D predictions. Based on the detailed mechanism, Wu *et al.* [18] proposed a reduced chemical reaction mechanism for modelling the mixed combustion of saturated furans (tetrahydrofuran, 2-methyltetrahydrofuran and 2-BTHF). The accuracy of the newly developed mechanism was verified by comparing the predictions of ignition delay times, speciation profiles and laminar flame speeds for the three tetrahydrofuran fuel compositions with experimental measurements in the literature.

To fill this gap, the primary objective of this work is to develop a reduced reaction mechanism for 2-BTHF. Based on this mechanism, a corresponding mechanism applicable to 2-BTHF/n-heptane/toluene fuels is created to numerically simulate the combustion of 2-BTHF/diesel blends, with the aim of studying the effect of blending 2-BTHF in diesel. Experimental data of ignition delay times and laminar flame speeds for the single-component fuels [14, 19-25] (2-BTHF, n-heptane, and toluene) and the binary-component fuels [26, 27] (n-heptane/toluene) under this mechanism were validated separately. In addition, the effect of blending different proportions of 2-BTHF in diesel on its combustion characteristics is investigated. Satisfactory results were obtained when using this reduced reaction mechanism to predict the above-mentioned physical quantities.

2. Mechanism construction

2.1. Mechanism construction strategy

The strategy for constructing a reduced reaction mechanism for 2-BTHF/n-heptane/toluene is shown in Figure 1. At the beginning of the study, proven mechanism reduction techniques were applied to reduce the detailed reaction mechanism of 2-BTHF proposed by Cai *et al.* [14]. Due to the complex composition of diesel, n-heptane and toluene were selected as alternative fuels to diesel, and their respective reaction mechanisms were coupled with the reduced 2-BTHF mechanism. The reduced mechanism was then optimized using sensitivity analysis, and the optimized mechanism was thoroughly verified with extensive experimental data. After the above steps, the reduced reaction mechanism of 2-BTHF/n-heptane/toluene was successfully established.

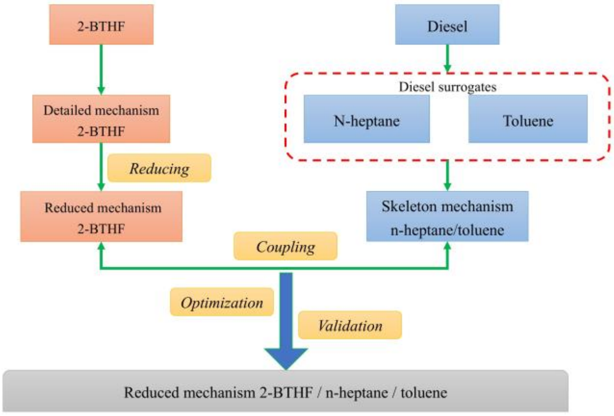

Figure 1. The mechanism development process

2.2. The reduced 2-BTHF mechanism

A detailed mechanism for 2-BTHF consisting of 424 species and 1790 reactions was proposed by Cai *et al.* [14]. This mechanism has been validated against experimental data under engine-relevant conditions, demonstrating high predictive accuracy. Consequently, it was adopted in the current study. However, due to its extensive size, a reduction process was necessary.

In the initial reduction stage, the Direct Relation Graph with Error Propagation (DRGEP) method and the isomer lumping method were employed. Based on the error propagation theory, the DRGEP method can accurately identify and eliminate decoupled species and irrelevant reactions within an acceptable error range, which have little impact on the overall reaction process. The isomer lumping method, on the other hand, decreases the complexity of the reaction system by reducing the number of species. It does so by grouping isomers with similar chemical structures. Subsequently, the sensitivity analysis method [28] was used to further optimize the initially reduced mechanism. Sensitivity analysis can identify the reactions and species that play a crucial role in the reaction process. By adjusting and optimizing these key factors, the performance of the mechanism was further improved. Through the above-mentioned steps, a reduced version of the 2-BTHF reaction mechanism was finally obtained, which contains only 42 species and 145 reactions. Figure 2. provides a detailed illustration of the reduction process of the 2-BTHF mechanism.

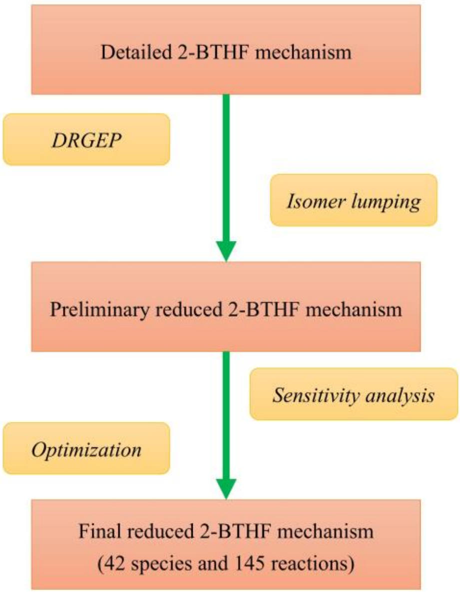

Figure 2. The flowchart of 2-BTHF reduced mechanism construction

2.2.1 *DRGEP and isomer lumping*

The DRGEP method possesses the capacity to eliminate a substantial number of superfluous species and reactions. As such, it is often utilized as a preliminary step in the process of mechanism reduction [29]. The fundamental principle behind this method involves identifying the optimal pathway by focusing on the target species A, and determining the importance coefficients of other components relative to species A. A threshold is then established, and only those components whose importance coefficients surpass this threshold are retained. The direct inter-species interaction coefficients for these retained components are as follows:

$$r_{\mathrm{AB}} = \frac{\left|\sum_{i=1}^{n_{\mathrm{R}}} \nu_{\mathrm{A},i}\omega_i\delta_{\mathrm{B}}^i\right|}{max\left[\sum_{i=1}^{n_{\mathrm{R}}} \max\left(0,\nu_{\mathrm{A},i}\omega_i\right),\sum_{i=1}^{n_{\mathrm{R}}} \max\left(0,-\nu_{\mathrm{A},i}\omega_i\right)\right]} \tag{1}$$

where ω_i is the net reaction rate of the ith elementary reaction, $\nu_{\mathrm{A},i}$ is the stoichiometric coefficient of species A in the ith elementary reaction, and n_{R} denotes the total number of elementary reactions. The coefficient δ_{B}^i is associated with species B. where if the i elementary reaction contains component B, then $\delta = 1$, otherwise $\delta = 0$. The path-dependence coefficient is given by:

$$r_{AB,P} = \prod_{J=1}^{n-1} r_{S_J S_{J+1}} \tag{2}$$

$$R_{\mathrm{AB}} = \max_{\text{all path p}} \left(r_{\mathrm{AB,P}} \right) \tag{3}$$

Where $S_1 = A$, $S_2 = B$, and R_{AB} represents the final expression for the coefficient of importance among species. Simultaneously, a substantial number of isomers are incorporated within the detailed mechanism, particularly noticeable during the low-temperature reaction phase [30]. Given that the isomeric species have the same molar mass and similar thermodynamic properties and transport parameters, they can be combined into a single representative species. This allows for the integration of their participation in the elementary reactions into a single backbone reaction pathway, thus further optimizing and reducing the size of the mechanism.

During the reduction phase of the DRGEP method and the process of isomer lumping, 2-BTHF, water (H_2O), hydroxide (OH), carbon monoxide (CO), carbon dioxide (CO_2), hydrogen (H_2), oxygen (O_2), and nitrogen (N_2) were chosen as target species. These small molecular species play a crucial role in the combustion process, typically exhibiting high stability and rapid reaction rates. By preserving these small molecules during the mechanism reduction, a more comprehensive understanding of the overall trends and characteristics of the combustion reaction can be achieved. Table 1. provides the specifics of the reduced mechanism working conditions.

Table 1. Reduced Mechanism Working Conditions

Pressure (bar)	Temperatures (K)	equivalence ratios	Target species
10-20	650-1500	0.5-2	2-BTHF, H_2O, OH, CO, CO_2, H_2, O_2, N_2

The ignition delay and laminar flame processes of 2-BTHF were comprehensively simulated through the closed homogeneous batch reactor module and the premixed laminar flame Speed module in the CHEMKIN-PRO software [31]. Figure 3 displays comparisons between the experimental data [14] and the predicted ignition delay times and laminar flame speeds of 2-BTHF/air mixtures using the mechanism after the initial reduction stage, with symbols denoting the experimental data and solid lines representing the predicted data generated by origin software.

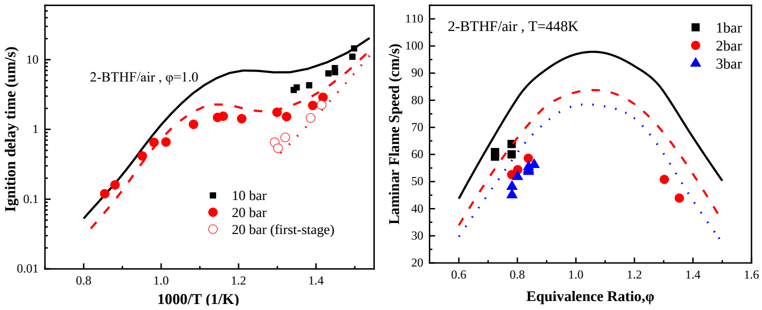

(a) (b)

Figure 3. Comparisons of the ignition delay times and laminar flame speeds of 2-BTHF predicted by experimental data (symbols) and optimized mechanism (lines). Closed and open symbols denote experimental total and first-stage ignition delay times, respectively

2.2.2 Optimization of reaction rate coefficients

The initial reduction of the mechanism has led to a significant reduction in its size and accurate prediction of experimental data for total ignition delay time at different pressures as well as experimental data for first-stage ignition delay time at 20 bar. However, this mechanism obviously overestimates the laminar flame speeds, particularly the data obtained under low-temperature conditions. Consequently, it is imperative to optimize the mechanism. The specific approach involves refining the reaction parameters to adjust the reaction rates, thereby enhancing prediction accuracy. Notably, all the reaction rates are characterized by the Arrhenius Eq. 4.

$$K_i = A_i T^{b_i} \exp\left(-\frac{E_i}{RT}\right) \quad for\ i = 1, \dots N_R \tag{4}$$

where A_i represents the pre-exponential factor, T represents the temperature, b_i represents the temperature exponent, E_i represents the activation energy, N_R represents the number of reactions, and R= 8314.3J/mol K is the universal gas constant. The A_i represents the frequency of molecular collisions and is categorized as an empirical constant [32]. For varying ranges of applicability, it assumes different values. The E_i is determined by factors such as molecular structure and is typically ascertained through experimental means, without subsequent adjustment. Therefore, during the optimization of the mechanism, the A_i is often adjusted. To identify which specific reactions require adjustment, sensitivity analysis can be conducted to pinpoint the partial reactions with the highest sensitivity to the mechanism. Subsequently, adjusting the A_i of these reactions can achieve the objective of mechanism optimization. The sensitivity analysis involves examining how variations in the rate constant of each reaction within a system impact the system's characteristic quantity under specified operating conditions. By comparing the sizes of sensitivity coefficients, one can ascertain the relative importance of each elementary reaction. This allows for the omission of insignificant reactions and the adjustment of reaction rate constants for critical reactions, thereby achieving the goal of mechanism optimization. The expression for the sensitivity coefficient is:

$$\tilde{S} = \frac{k_j}{y^i}\frac{\partial y^i}{\partial k_j} = \frac{\partial lnc_i}{\partial lnk_j} \tag{5}$$

Where $\tilde{S}$ represents the sensitivity coefficient, k_j is the reaction rate constant of the jth elementary reaction within the detailed mechanism, y^i denotes a particular variable in the system (such as concentration, temperature, etc.). The sensitivity of the variable y^i to the rate constant k_j of a specific elementary reaction is quantified by $\tilde{S}$. A larger value of $\tilde{S}$ indicates that the elementary reaction in question has a more significant influence on the variable y^i [33].

During the optimization of the laminar flame speeds of 2-BTHF, deviations between the simulated values and experimental values were observed for equivalent ratios close to 0.8, especially under pressures ranging from 1 to 3 bar across all three tested conditions. Therefore, a sensitivity analysis of 2-BTHF was carried out using the CHEMKIN-PRO software [31] under the conditions of 1-3 bar pressure and an equivalence ratio of 0.8. This analysis identified the reactions that had the most significant impact on the laminar burning velocity of 2-BTHF and determined the sensitivity coefficients of each reaction. Reactions with positive sensitivity coefficients enhance the laminar flame speed, while those with negative sensitivity coefficients inhibit it. Subsequently, the A_i of these elementary reactions in the 2-BTHF mechanism file were manually modified to achieve the purpose of mechanism optimization. Figure 4 shows the results of the sensitivity analyses conducted at pressures ranging from 1 to 3 bars and an equivalence ratio of 0.8. The graph reveals that reactions R (10), R (55), R (26), R (51), and R (8) significantly influence the conditions within this pressure range. Specifically, reactions R (10) and R (55) exhibit positive sensitivity coefficients, indicating that they enhance the laminar flame speed, whereas reactions R (26), R (51), and R (8) display negative sensitivity coefficients, indicating that they inhibit laminar flame speed.

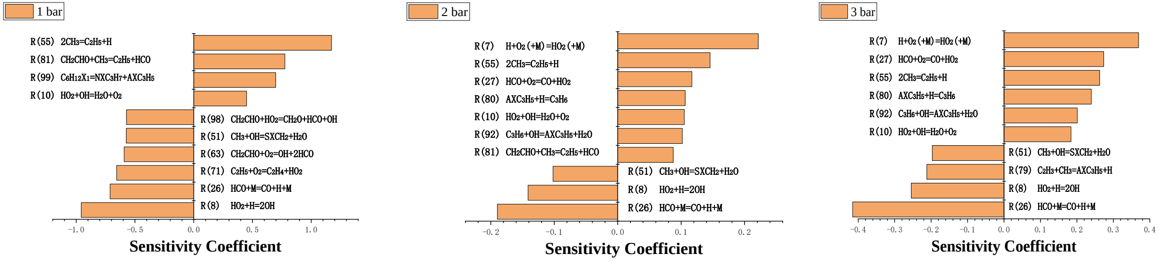

(a) (b) (c)

Figure 4. Sensitivity analysis for laminar flame speed of 2-BTHF at different pressures

Given that the simulated values constantly surpass the experimental ones [14], the adjustment approach is as follows. For reactions having positive sensitivity coefficients like R (10) and R(55), the rate constants A_i should be decreased. This will slow down the reaction rate, ultimately leading to a reduction in the laminar burning rate. On the contrary, for reactions with negative sensitivity coefficients such as R (26), R (51), and R(8), the rate constant A_i should be increased. This will speed up the reaction rate, and as a result, decrease the laminar burning rate. After several adjustments of the A_i, the mechanism after each adjustment was simulated and compared with the experimental data [14] of the laminar flame speeds of 2-BTHF. After finding the most suitable optimized value of A_i, the results are listed in Tab. 2.

Table 2. Improvement of the rate constants in the 2-BTHF mechanism

Chemical reactions	Original A_i	Adjusted A_i
R (10) $HO_2+OH=H_2O+O_2$	3.89E+14	2.89E+13
R (55) $2CH_3=C_2H_5+H$	6.52E+13	6.84E+12
R (26) $HCO+M=CO+H+M$	3.47E-10	3.0E-11
R (51) $CH_3+OH=SXCH_2+H_2O$	3.22E+16	6.44E+17
R (8) $HO_2+H=2OH$	7.079E+12	7.079E+13

During the optimization of the mechanism using sensitivity analysis, several secondary reactions with low sensitivity coefficients were identified and removed, as they had a negligible impact on the combustion characteristics of 2-BTHF. This step further reduced the mechanism. The final reduced 2-BTHF mechanism includes 42 species and 145 reactions.

The 2-BTHF reaction mechanism initially reduced by the DRGEP and isomer lumping method exhibits moderate predictive capability for ignition delay times but overestimates the laminar flame speed, particularly under low-temperature conditions (as shown in Fig. 3). In contrast to WU *et al*. [18], who developed a three-component mechanism for the furan family without reducing it for single 2-BTHF, the optimized mechanism in Fig. 5 predicts ignition delay times and laminar flame speeds more accurately—especially under oxygen-enriched conditions, where it outperforms WU’s mechanism in laminar flame speed prediction. The sensitivity analysis and adjustment of reaction rate coefficients during optimization enhance its accuracy, allowing the optimized mechanism to better reflect experimental data [14] and verifying the effectiveness of the optimization method.

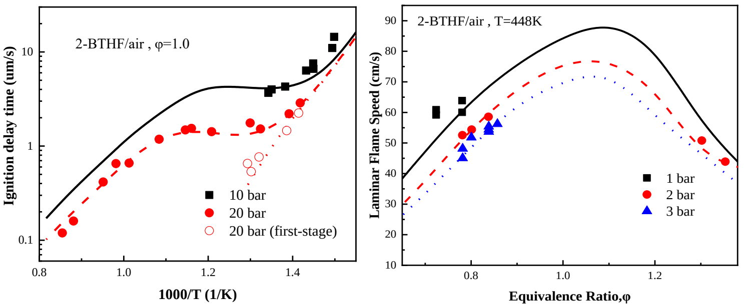

(a) (b)

Figure 5. Comparisons of the ignition delay times and laminar flame speeds of 2-BTHF predicted by experimental data (symbols) and optimized mechanism (lines). Closed and open symbols denote experimental total and first-stage ignition delay times, respectively

2.3. Mechanism combination

The reduced mechanisms of n-heptane, toluene, and 2-BTHF were integrated through the decoupling approach to develop a comprehensive three-component mechanism. The decoupling method classifies the mechanism into three segments: a detailed sub-mechanism for C_0-C_1 hydrocarbons, a reduced sub-mechanism for C_2-C_3 hydrocarbons, and a skeletal fuel-specific sub-mechanism. By coupling the corresponding sub-mechanisms, the skeletal mechanism of the mixture fuels is formed. In our previous work [13], the decoupling approach is very effective in integrating the fuel mechanism and allows for a more rational delineation of the reaction mechanism. The sub-mechanisms of n-heptane and toluene were sourced from reference [34], while the sub-mechanism of 2-BTHF was derived from the newly reduced 2-BTHF mechanism. Additionally, the reduced C_2-C_3 sub-mechanism and the detailed H_2/CO/C_1 mechanism were further incorporated into these sub-mechanisms, thereby finalizing the reaction pathway [35]. The schematic reaction pathway of the 2-BTHF/n-heptane/toluene mechanism is illustrated in Fig. 6.

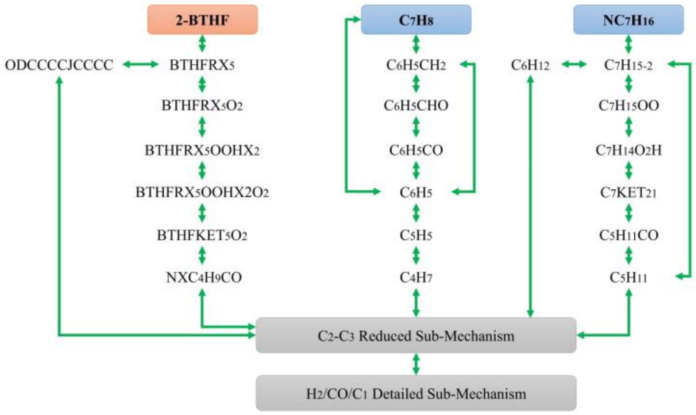

Figure 6. The schematic reaction pathway for the 2-BTHF/n-heptane/toluene mechanism

2.4. Mechanism optimization

Following the decoupling process, the combined three-component mechanism requires optimization to minimize the differences between the predictions and experimental results [14, 19-25]. The adjusted A_i values in Tab. 3 were determined through sensitivity analysis of the coupled 2-BTHF/n-heptane/toluene mechanism. First, the key reactions in the mechanism that significantly influence the combustion characteristics were identified. Then, an analysis was conducted on how changes in the rate constants A_i of these reactions affect the behavior of the entire system. If a reaction has a positive sensitivity coefficient for a specific combustion characteristic, increasing its A_i value will enhance the reaction's impact on that characteristic. Conversely, for reactions with negative sensitivity coefficients, decreasing the A_i value will produce the desired effect. After multiple simulations and adjustments, the values that minimized the differences between the mechanism's predicted results and the experimental data were selected as the adjusted A_i values to ensure the accuracy of the mechanism in predicting combustion behavior. For the sake of brevity, this process is not detailed here, and the specific adjustment methods can be found in the 2-BTHF sensitivity analysis described above. Finally, the mechanism for 2-BTHF/n-heptane/toluene (consisting of 78 species and 300 reactions) was obtained.

Table 3. Improvement of the rate constants in the combined mechanism

Chemical reactions	Original A_i	Adjusted A_i
R (9) $C_7H_{14}O_2H+O_2=C_7H_{14}O_4H$	4.6E+12	4.6E+11
R (28) $C_6H_5+H=C_6H_6$	4.0E+14	2.2E+14
R (119) $HO_2+H=2OH$	7.079E+13	1.0E+12
R (133) $CO+OH=CO_2+H$	2.229E+5	1.5E+5
R (156) $CH_3+HO_2=CH_3O+OH$	5.0E+11	1.0E+12
R (250) $HOCHO+OH=H_2O+CO_2+H$	4.62+E6	2.62+E6

3. Result and discussion

3.1. Mechanism validations

The mechanism’s capacity to precisely predict ignition delay times and laminar flame speeds serves as a crucial indicator of its effectiveness in describing reaction kinetics. In this research, comprehensive simulations of both the entire ignition delay and laminar flame processes was conducted by means of the closed homogeneous batch reactor module and the premixed laminar flame speeds calculation module within software [31].

3.1.1 Ignition delay time

Predicted and Experimental [14, 21-23, 27] ignition delay times for 2-BTHF/air, n-heptane/air, toluene/air and n-heptane/toluene/air mixtures were compared under different operating conditions to assess the performance of the different mechanisms. As shown in the predicted results of the mechanism depicted in Fig. 7(a), the ignition delay time of 2-BTHF increases gradually with decreasing temperature. This trend is attributed to the reduction in activation energy caused by the temperature drop, which is highly consistent with the experimental data [14]. Meanwhile, this mechanism accurately simulates the variation in the negative temperature coefficient region near the equivalence ratio of 1.2-1.3. For the prediction results of n-heptane, under various equivalence ratios and pressures, this mechanism accurately reproduces the relationship between the ignition delay times of n-heptane and pressure. It effectively captures the trend where a decrease in pressure results in higher ignition delay times [36], which align closely with the experimental values reported in [22, 23], as illustrated in Figs. 7(b) and (c). In the prediction scenario for toluene, Fig. 7(d) and (e) present a comparison between the experimental data of toluene/air under varying conditions and the predicted results of this mechanism. When the equivalence ratio is 1, the mechanism accurately reproduces the experimental values [21] of toluene at pressures of 12 atm and 50 atm. Despite some discrepancies between the mechanism and experimental values at a pressure of 50 atm and equivalence ratios from 0.25 to 0.5, the overall trend remains in line with the experimental observations. Finally, Fig. 7(f) shows the predicted ignition delay times for n-heptane/toluene/air mixtures (with a molar composition of 35% n-heptane and 65% toluene) under lean premix condition (equivalence ratio = 0.3) at two different pressures, which are very consistent with the experimental data from Herzler *et al.*[27].

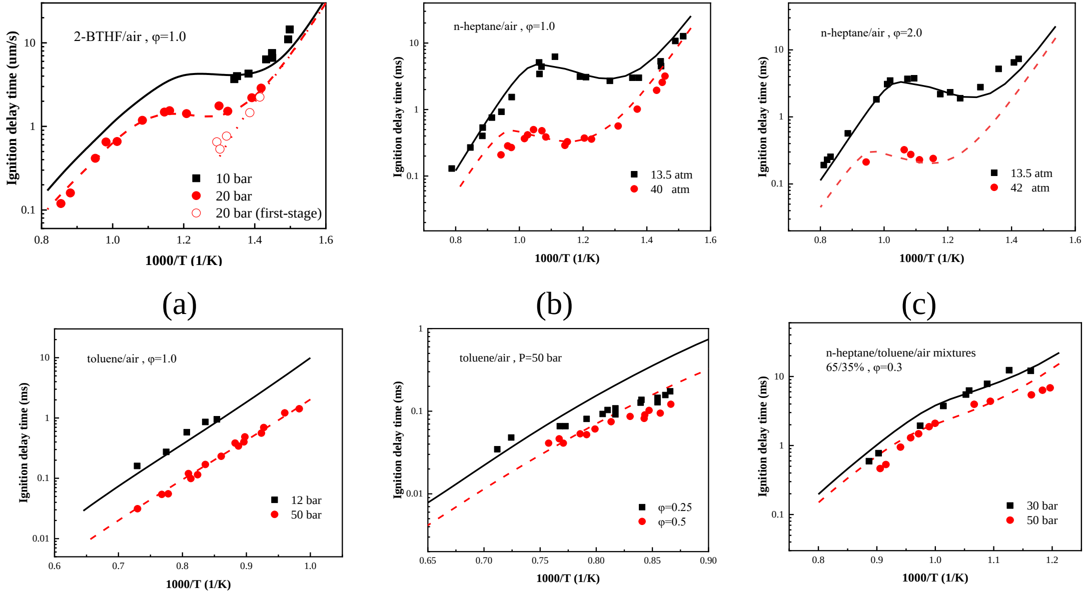

(a) (b) (c)

(d) (e) (f)

Figure 7. Comparison of ignition delay times between predictions (lines) and experiments (symbols) for various fuel/air mixtures

3.1.2 Laminar flame speeds

As shown in Fig. 8, the laminar flame speeds of 2-BTHF/air, n-heptane/air, toluene/air and diesel/air mixtures are presented across various equivalence ratios. The mechanism-predicted data demonstrates a high degree of agreement with the experimental data. Specifically, Fig. 8(a) highlights the remarkable agreement between the predicted data and the experimental data of 2-BTHF [14] across varying pressures. This mechanism accurately captures the combustion behavior, providing a precise representation of the underlying processes. Figure 8(b) illustrates the laminar flame speeds of n-heptane at different temperatures, revealing a consistent trend of increasing flame speed with increasing initial temperature. This trend aligns with the findings of Kumar *et al.* [20], with discrepancies between experimental and predicted values remaining within 5%. Figure 8(c) presents a comparison between experimental observations from Jerzembeck *et al.* [19] and the model. Notably, at ambient temperature, an increase in initial pressure corresponds to a decrease in laminar flame speeds. The laminar flame speeds predicted by the mechanism reach their peak values at an equivalent ratio of around 1.1. The corresponding peak values are 26.6 cm/s, 21.4 cm/s, and 18 cm/s, respectively. Although there is a slight deviation from the experimental data, which may be attributed to the mixture containing 2-BTHF, the overall consistency remains strong. Figures 8(d) and (e) exhibit a comparison of the variations in laminar flame speeds of toluene with experimental data reported by Hui and Sung [25] and Sileghem *et al.* [24], respectively. The observed behavior of laminar flame speed in toluene is analogous to that of n-heptane in terms of temperature and pressure variations, showing a close alignment with the experimental data in both instances. Consequently, given the high degree of agreement, further detailed discussion on this similarity is deemed unnecessary at this juncture. Figure 8(f) contrasts the laminar flame speeds of diesel fuel predicted by the proposed mechanism with experimental data [26] at a pressure of 1 atm and a temperature of 470K. Despite the presence of minor discrepancies under lean premixed conditions, when considering the experimental errors as well as the disparities in species and composition between the diesel surrogate fuel (35% n-heptane and 65% toluene) and actual diesel fuel, the consistency between the predicted and experimental outcomes can be regarded as satisfactory.

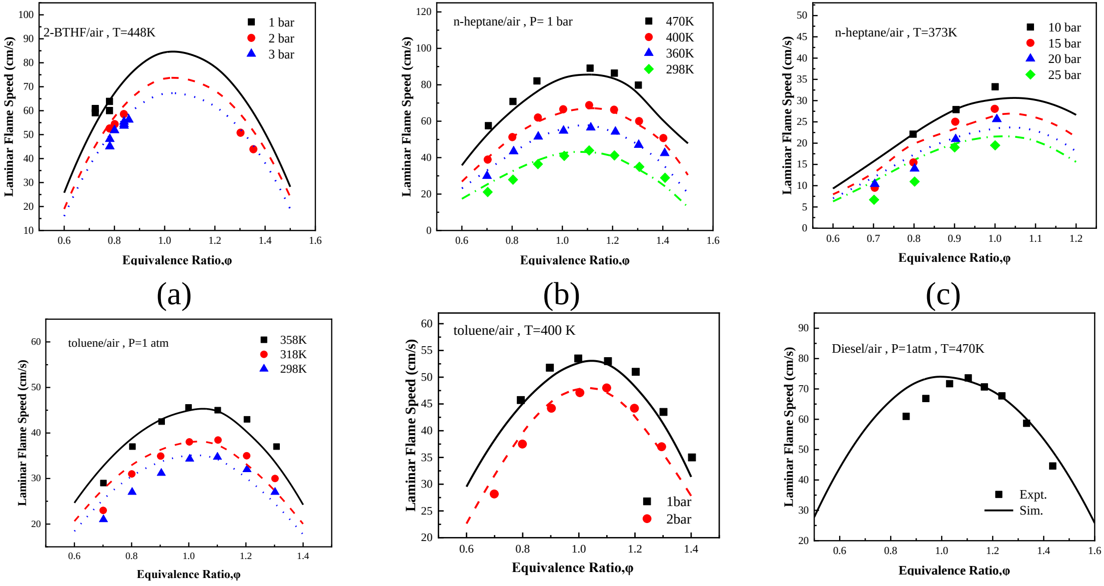

(a) (b) (c)

(d) (e) (f)

Figure 8. Comparison of laminar flame speeds between predictions (lines) and experiments (symbols) for various fuel/air mixtures

Overall, the chemical kinetic model accurately captures the trends in ignition delay times and laminar burning velocities for each component across varying operating conditions, demonstrating an excellent agreement with the experimental results.

3.2. Effect of 2-BTHF addition on the combustion characteristics of diesel fuel

To investigate the effect of 2-BTHF on the combustion characteristics of diesel, this study conducted blending experiments where 2-BTHF was mixed into diesel at varying proportions, ranging from 0 to 30%. As was the case in the study conducted by Heng *et al.* [36], the objective of the present study was to predict the trend in how the addition of 2-BTHF alters the combustion characteristics of diesel. The specific proportions of fuel components used in these blends are detailed in Tab. 4.

Table 4. Molar fractions of major components (%)

Fuel	A	B	C	D
N-heptane (%)	35	31.5	28	24.5
Toluene (%)	65	58.5	52	45.5
2-BTHF (%)	0	10	20	30

Figure 9 shows the comparison of the predicted values of 2-BTHF/n-heptane/toluene coupling mechanisms with the experimental values [26, 27] of diesel fuel for ignition delay time and laminar ignition velocity at different 2-BTHF blending ratios. As illustrated in Fig. 9(a), the incorporation of varying proportions of 2-BTHF exhibits a minimal effect on ignition delay time. This observation can be attributed to the significance of DCN as a crucial indicator for evaluating the ignition performance of diesel in compression ignition engines. A higher DCN implies enhanced ignition characteristics, manifesting as a shorter ignition delay, more homogeneous combustion, and a smoother engine startup. Notably, The DCN of 2-BTHF is comparable to that of diesel. Consequently, blending 2-BTHF with diesel has an insignificant effect on ignition delay time.

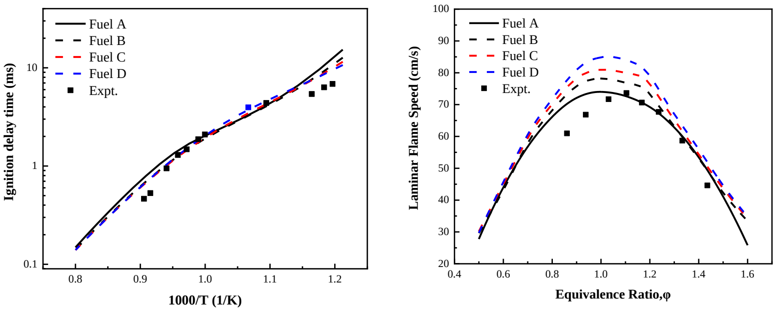

(a) (b)

Figure 9. Comparisons of ignition delay times and laminar flame speeds for diesel/air mixtures under different blending proportions of 2-BTHF

As shown in Fig. 9(b), the laminar flame speeds present a consistent upward trend. Moreover, the most remarkable impact on the peak laminar flame speeds occurs with the increase in the proportion of 2-BTHF. This phenomenon can be attributed to the lower boiling point of 2-BTHF compared to diesel, leading to a higher evaporation rate. Upon entering the combustion chamber, the low-boiling-point fuel rapidly evaporates and mixes with air, creating optimal combustion conditions and accelerating the laminar flame speed. Furthermore, as an oxygen-containing fuel, 2-BTHF provides additional oxygen during combustion, promoting more complete fuel oxidation, enhancing combustion efficiency, and ultimately resulting in an accelerated laminar flame speed.

4. Conclusions

In this paper, the reduced mechanism of 2-BTHF was initially developed and optimized through DRGEP, isomer lumping, and sensitivity analysis. Compared with the detailed mechanism, the reduced one comprising 42 species and 145 reactions can fulfill the requirement for efficient prediction. It was then combined with the diesel surrogate mechanism, effectively addressing the issues of complex mechanism and high computational cost. Subsequently, a reduced chemical kinetic mechanism of 2-BTHF/n-heptane/toluene was put forward to achieve the prediction of the combustion characteristics of the blended fuel. Next, by investigating the combustion characteristics, the key reactions were identified and optimized, resulting in the final mechanism with 78 species and 300 reactions. This three-component mechanism was thoroughly verified by experimental data, including ignition delay times and laminar flame speeds under diverse working conditions. Eventually, the research findings indicated that blending 2-BTHF would steadily increase the laminar flame speeds of diesel while having a minimal impact on the ignition delay time. In general, the mechanism constructed in this study can excellently reproduce experimental data under various working conditions and shows excellent potential for simulating the combustion of 2-BTHF/n-heptane/toluene blended fuels.

References

[1] Zhu, J., *et al.*, Autoignition behavior of methanol/diesel mixtures: Experiments and kinetic modeling, *Combustion and Flame*, *228* (2021), pp. 1-12

[2] Lin, Q., *et al.*, Development of a compact and robust Polyoxymethylene Dimethyl Ether 3 reaction mechanism for internal combustion engines, *Energy Conversion and Management*, *185* (2019), pp. 35-43

[3] Mohan, B., *et al.*, Experimental study of spray characteristics of biodiesel derived from waste cooking oil, *Energy Conversion and Management*, *88* (2014), pp. 622-632

[4] Wang, H., *et al.*, Development of a reduced chemical kinetic mechanism for ammonia/diesel combustion over a wide range of ammonia energy ratios, *Fuel*, *381* (2025), p. 133536

[5] Ali Abuelnour, M., *et al.*, Numerical investigation of hydrogen-diesel dual fuel engine: Combustion and emissions characteristics under varying hydrogen concentration and exhaust gas recirculation, *Fuel*, *377* (2024), p. 132794

[6] Lin, Q., *et al.*, Auto-ignition of polyoxymethylene dimethyl ether 3 (PODE3) blended with diesel and gasoline via combustion under homogeneous charge compression ignition, *Energy Conversion and Management: X*, *11* (2021), p. 100093

[7] Li, S., *et al.*, Development of a reduced n-heptane/toluene/tetrahydrofuran mechanism for dual-fuel engine combustion prediction, *Fuel*, *326* (2022), p. 124914

[8] Wang, H., *et al.*, Development of an n-heptane-n-butanol-PAH mechanism and its application for combustion and soot prediction, *Combustion and Flame*, *160* (2013), 3, pp. 504-519

[9] Ulonska, K., *et al.*, Screening pathways for the production of next generation biofuels, *Energy & Fuels*, *30* (2016), 1, pp. 445-456

[10] Wei, M., *et al.*, Development and validation of a reduced MF/biodiesel mechanism for diesel engine application, *Thermal Science*, *27* (2023), 2 Part B, pp. 1465-1477

[11] Zhang, T., *et al.*, Construction and validation of a reduced mechanism in a diesel engine fueled with 2-methylfuran-diesel, *Thermal Science*, *27* (2023), 2 Part B, pp. 1495-1505

[12] Sudholt, A., *et al.*, Ignition characteristics of a bio-derived class of saturated and unsaturated furans for engine applications, *Proceedings of the Combustion Institute*, *35* (2015), 3, pp. 2957-2965

[13] Chen, K., *et al. Development of n-heptane/2-butyltetrahydrofuran mechanism based on decoupling approach*,Journal of Physics: Conference Series,2024,2683, p. 012008

[14] Cai, L., *et al.*, Experimental and numerical study of a novel biofuel: 2-Butyltetrahydrofuran, *Combustion and Flame*, *178* (2017), pp. 257-267

[15] Xu, N., *et al.*, Review on the production methods and fundamental combustion characteristics of furan derivatives, *Renewable and Sustainable Energy Reviews*, *54* (2016), pp. 1189-1211

[16] Guan, C., *et al.*, Effects of oxygenated fuels on the particle-phase compounds emitted from a diesel engine, *Atmospheric Pollution Research*, *8* (2017), 2, pp. 209-220

[17] Rudolph, T., Thomas J., NOx, NMHC and CO emissions from biomass derived gasoline extenders, *Biomass*, *16* (1988), 1, pp. 33-49

[18] Wu, S., *et al.*, Development of a highly compact and robust chemical reaction mechanism for the oxidation of tetrahydrofurans under engine relevant conditions, *Fuel*, *276* (2020), p. 118034

[19] Jerzembeck, S., *et al.*, Laminar burning velocities at high pressure for primary reference fuels and gasoline: Experimental and numerical investigation, *Combustion and Flame*, *156* (2009), 2, pp. 292-301

[20] Kumar, K., *et al.*, Laminar flame speeds of preheated iso-octane/O2/N2 and n-heptane/O2/N2 mixtures, *Journal of propulsion and power*, *23* (2007), 2, pp. 428-436

[21] Hartmann, M., *et al.*, Auto-ignition of toluene-doped n-heptane and iso-octane/air mixtures: High-pressure shock-tube experiments and kinetics modeling, *Combustion and Flame*, *158* (2011), 1, pp. 172-178

[22] Luo, J., *et al.*, Experimental and numerical study on suitable diesel fuel surrogates in low temperature combustion conditions, *Fuel*, *97* (2012), pp. 621-629

[23] Ciezki, H.K., Adomeit G., Shock-tube investigation of self-ignition of n-heptane-air mixtures under engine relevant conditions, *Combustion and Flame*, *93* (1993), 4, pp. 421-433

[24] Sileghem, L., *et al.*, Laminar burning velocity of gasoline and the gasoline surrogate components iso-octane, n-heptane and toluene, *Fuel*, *112* (2013), pp. 355-365

[25] Hui, X., Sung C.-J., Laminar flame speeds of transportation-relevant hydrocarbons and jet fuels at elevated temperatures and pressures, *Fuel*, *109* (2013), pp. 191-200

[26] Chong, C.T., Hochgreb s., Measurements of laminar flame speeds of liquid fuels: Jet-A1, diesel, palm methyl esters and blends using particle imaging velocimetry (PIV), *Proceedings of the Combustion Institute*, *33* (2011), 1, pp. 979-986

[27] Herzler, J., *et al.*, Shock-tube study of the autoignition of n-heptane/toluene/air mixtures at intermediate temperatures and high pressures, *Combustion and Flame*, *149* (2007), 1, pp. 25-31

[28] Turanyi, T., *et al.*, Reaction rate analysis of complex kinetic systems, *International Journal of Chemical Kinetics*, *21* (1989), 2, pp. 83-99

[29] Pepiot-Desjardins, P., Pitsch H., An efficient error-propagation-based reduction method for large chemical kinetic mechanisms, *Combustion and Flame*, *154* (2008), 1-2, pp. 67-81

[30] Pepiot-Desjardins, P., Pitsch H., An automatic chemical lumping method for the reduction of large chemical kinetic mechanisms, *Combustion Theory and Modelling*, *12* (2008), 6, pp. 1089-1108

[31] DESIGNS, M.E., Chemkin-pro, *Ansys*. (2011)

[32] Laidler, K.J., The development of the Arrhenius equation, *Journal of chemical Education*, *61*. (1984), 6, p. 494

[33] Glassman, I., *et al.*, *Combustion*. Academic press, 2014

[34] Li, S., *et al.*, Development of a phenomenological soot model integrated with a reduced TRF-PAH mechanism for diesel engine application, *Fuel*, *283* (2021), p. 118810

[35] Chang, Y., *et al.*, Development of a skeletal mechanism for diesel surrogate fuel by using a decoupling methodology, *Combustion and Flame*, *162* (2015), 10, pp. 3785-3802

[36] Heng, Y., *et al.*, High-pressure ignition behaviors of methane/ethane/propane-n-heptane mixtures representing natural gas-diesel dual fuel, *Thermal Science*, *28* (2024), 1 Part A, pp. 115-132

Submitted: 16.02.2025.
Revised: 26.06.2025.
Accepted: 30.06.2025.